



AUTHOR(S):

TITLE:

YEAR:

Publisher citation:

OpenAIR citation:

Publisher copyright statement:

This is the _____ version of an article originally published by _____
in _____
(ISSN _____; eISSN _____).

OpenAIR takedown statement:

Section 6 of the "Repository policy for OpenAIR @ RGU" (available from <http://www.rgu.ac.uk/staff-and-current-students/library/library-policies/repository-policies>) provides guidance on the criteria under which RGU will consider withdrawing material from OpenAIR. If you believe that this item is subject to any of these criteria, or for any other reason should not be held on OpenAIR, then please contact openair-help@rgu.ac.uk with the details of the item and the nature of your complaint.

This publication is distributed under a CC _____ license.

Preparation and analysis of multi-layered hybrid nanostructures

**Prashant S. Khobragade¹, D.P. Hansora¹, JitendraB. Naik¹, James Njuguna²,
Satyendra Mishra^{1*}**

*¹University Institute of Chemical Technology, North Maharashtra University,
Jalgaon-425001, Maharashtra, India*

*²School of Engineering, Robert Gordon University, Riverside East,
Aberdeen, AB10 7GJ, United Kingdom*

*Corresponding author's Email address: profsm@rediffmail.com

Tel.: +91-257-2258420. Fax: +91-257-2258403

Abstract

In this study, we report a simple and efficient (bath ultrasonication) method for the preparation of multi-functional layered hybrid nanostructures using graphene oxide (GO) and modified Mg-Al layered double hydroxides (LDH) [LDH@GO]. The functional composition, crystalline nature, layered surface morphology and thermal behavior of the hybrid nanostructures of LDH@GO were characterized by Fourier transform infrared spectroscopy, X-ray diffraction, Field-emission scanning electron microscopy, Transmission electron microscopy, elemental analysis and thermo gravimetric analysis. The results confirmed the formation of layered hybrid nanostructures of LDH@GO showing a significant increment in the spacing between GO sheets due to the incorporation of LDH. Also hybrid nanostructures of LDH@GO have better thermal stability as compared to pristine GO.

Keywords: Graphene oxide, Layered double hydroxide, Surface modification, Hybrid nanostructures, Properties.

1. Introduction

The field of material science and nanotechnology has blossomed over the last two decades due to various applications from medical to industrial sectors and from laboratory to market (Das and Prusty et al., 2013). But some of nanomaterials (NM) were observed with their aggregation due to the high specific area (Bourlinos et al., 2009; Mishra et al., 2010; Mali et al., 2012; Mishra et al., 2012; Esmaeili, et al., 2014; Angelopoulou et al., 2015) and also these NM were reported with specific use. On other side, alloying or hybridizing the two or more NM can give multifunctional properties of the resulting hybrid nanostructures (NS) and also they can be used in many applications. The combination of multi-dimensional NM or layered NS were used to prepare hybrid nanostructures with many advantages due to each kind of NM or NS (Bouakaz et al., 2015; Oraon et al., 2015; Alsharaeh et al., 2016; Chen et al., 2016; He 2016; Pérez del Pino et al., 2016, Kavinkumar et al., 2016; Zhao et al., 2016). These kinds of hybrid nanostructures with exceptional properties are effective and they were reported for the potential applications (Latorre-Sanchez et al., 2012; Lonkar et al., 2015). Many hybrid materials were reported, which can be made using different NS. But recently organic-inorganic hybrid NS have shown considerable attention (Mishra et al., 2010; Chatterjee et al., 2013). Among the various organic NS materials, graphene oxide (GO) has a tremendous interest in a scientific research. Because GO is two dimensional (2D) and conducting layered NM and it consists of one atom-thick planar sheets of sp^2 -bonded honeycomb structure of carbon atoms (Low et al., 2015). GO possesses extraordinary mechanical, thermal, electronic and physical properties, (Hansora et al., 2015; Lonkar et al., 2015), more importantly it contains a range of reactive oxygen

functional groups (e.g., hydroxyl groups) (Yan et al., 2016). Therefore, GO was used to prepare organic-inorganic hybrid NS (Wu et al., 2012; Nandi et al., 2013; Esmaeili et al., 2014; Yadav et al., 2014; Angelopoulou et al., 2015; Low et al., 2015; Jain et al., 2016). Many scientists have prepared hybrid NS using different metal and inorganic NM filled with GO, e.g., Titanium oxide–graphene (Heet al., 2016; Pérez del Pino et al., 2016; Zhao et al., 2016), Manganese-nickel mixed oxide/graphene (Latorre Sanchez et al., 2015), Organomontmorillonite/graphene (Bouakaz et al. 2015; Oraon et al., 2015), Calcium carbonate/GO (Zhou et al., 2016), Silver nanoparticle/GO (Kavinkumaret al., 2016), Cobalt oxide nanoparticles/reduced GO (Alsharaeh et al., 2016), Zinc oxide nanorods/graphene (Chen et al., 2016), Vanadium dioxide nano flowers decorated on GO (Kang et al., 2016) and novel boehmite/GO nano-hybrids (Zhanga et al., 2016). Graphene based polymer hybrid nanocomposites were also reported (Acharya et al., 2007; Das and Prusty et al., 2013; Nandi et al., 2013; Chakraborty et al., 2014; Yadav et al., 2014; Angelopoulou et al., 2015; Bouakaz et al. 2015; Oran et al., 2015; Yana et al., 2016). But recently in the field of inorganic NM, layered double hydroxide (LDH) has emerged as the most powerful NM for the preparation of multifunctional hybrids for various applications (Yuan et al., 2012). The LDH, a family member of inorganic layered NM, have recently attracted considerable attention because of their wide applications (Olf et al., 2009; Ladewig et al., 2010; Chakraborty et al., 2012; Yuan et al., 2012; Lonkar et al., 2013; Menezes et al., 2014; Yang et al., 2014; Zazoua et al., 2014). The chemical composition of LDH is generally described by the formula: $[M^{2+}_{1-x}M^{3+}_x(OH)_2]^{x+} [A^{n-}]_{x/n} \cdot mH_2O$. Usually, M^{2+} is a divalent metal (Ca^{2+} , Mg^{2+} , Zn^{2+} , Ni^{2+} , Co^{2+} , Mn^{2+} , Co^{2+} or Fe^{2+}), M^{3+} is a trivalent metal (Al^{3+} , Cr^{3+} , Mn^{3+} , Fe^{3+} , Co^{3+} or Ni^{3+}) and A^{n-} is a n -valent anion group (e.g. CO_3^{2-} , NO_3^- , PO_4^{3-} , SO_4^{2-} or Cl^-). The M^{2+}/M^{3+} ratio, also known as χ , usually lies in the range of $0.1 \leq \chi \leq 0.5$. LDH afford

space between the two layers and becomes suitable host for intercalation of planar transition metal complex catalyst containing porphyrin, phthalocyanine or Schiff base ligands (Sun et al., 2015). The LDH have a high anion exchange capacity and large surface area due to their structural configuration (Olf et al., 2009; Basu et al., 2014). The nanostructures of these minerals are brucite-like positively charged layers resulting from the partial substitution of original Mg^{2+} by Al^{3+} ions. The LDH can absorb inorganic as well as organic anions, which make them attractive materials for technological applications in different areas (Olf et al., 2009). Recently, graphene decorated layered metal hydroxides like LDH (with different metal) compositions were studied in order to diminish their stacking interactions and to limit the aggregation in graphene nanosheets (Garcia-Gallastegui et al. 2012; Latorre-Sanchez et al., 2012; Tang et al., 2012; Wen et al., 2013; Lonkar et al., 2015). In the present study, we report a simple method for preparation of multifunctional hybrid NS of Mg-Al-LDH@GO by bath ultra-sonication technique. Multi-layered hybrids of LDH@GO were analyzed by Fourier transform infrared (FTIR) spectroscopy, X-ray diffraction (XRD), Field-emission scanning electron microscopy (FE-SEM), Transmission electron microscopy (TEM), Elemental analysis (EDX) and thermo gravimetric analysis (TGA) to investigate their functional composition, crystalline nature, layered surface morphology, elemental analysis and thermal behavior.

2. Experimental

2.1 Materials

For the synthesis of Mg-Al-LDH, magnesium nitrate ($Mg(NO_3)_2 \cdot 6H_2O$) and aluminium nitrate ($Al(NO_3)_3 \cdot 9H_2O$) (98% purity) were purchased from Rankem, India. Sodium carbonate (anhydrous), Sodium hydroxide and sodium dodecyl sulphate (SDS)

were also purchased from Rankem, India and Sigma Aldrich, India respectively. For the synthesis of graphene oxide (GO), fine powder of graphite (98% purity) was purchased from LobaChem, India. Hydrogen peroxide (H_2O_2), Sulfuric acid (H_2SO_4), hydrochloric acid (HCl), sodium nitrate ($NaNO_3$) were purchased from Merck, India, while potassium permanganate ($KMnO_4$) was purchased from Rankem, India. All the chemicals were of analytical reagent grade and used without any further purification. Double distilled water was used throughout the experiments.

2.2 Synthesis of LDH@GO hybrid nanostructures

LDH@GO based hybrid NS were easily prepared by one-pot microwave-assisted synthesis approach (Garcia-Gallastegui et al. 2012; Tang et al., 2012; Wen et al., 2013; Lonkar et al., 2015). GO was prepared from graphite average particle size of $< 20 \mu m$ by a modified Hummers method (Yadav et al., 2014; Jain et al., 2016) and another simple and fast route is microwave assisted approach (Yan et al., 2016). Ultrasonic bath (Bio-Techniques, India) was used to exfoliate GO sheets to make them individual sheets in an aqueous dispersion of water (Bourlinos, et al., 2009; Esmaili, et al., 2014). Magnesium and aluminum (Mg-Al) based LDH were synthesized using $Mg(NO_3)_2 \cdot 6H_2O$ and $Al(NO_3)_3 \cdot 9H_2O$ by standard co-precipitation and thermal crystallization method (Acharya et al., 2007). SDS was used as a surface modifying agent for functionalization of the LDH, because SDS contains negatively charged functionality and highly nucleophilic sites in their chemical structure of LDH. Hence it is easy to make hybrids using GO and LDH. The hybrids layered NS of LDH@GO were synthesized using bath ultrasonication technique. Same amount of LDH and GO (to keep mass ratio of 1:1) was taken in two different beakers and 50 mL of water was added in each beaker. The resulting dispersions were sonicated for 15 min, and then LDH solution was added drop wise to the GO solution during bath sonication. The

resulting mixture was sonicated for additional 30 min which resulted in a colloidal dispersion. The resulting dispersion of LDH@GO was allowed to settle down for 48 h. Finally, the resulting product was vacuum dried at 120°C, which removed any remaining traces of water.

2.3 Characterizations

The functional composition, crystalline nature, thermal behavior, surface and layered morphology, elemental composition and thermal behavior of GO sheets, LDH sheets and hybrid layered NS of LDH@GO hybrids were analyzed. The crystallinity was determined by X-ray diffractometer (XRD, Bruker D8 Advance, Berlin, Germany) in the range of 0-80°. The samples were placed vertically in front of the X-ray source. The detector was moving at an angle of 2θ , while the sample was moving at an angle of θ and the wavelength λ was 1.54 Å (Cu K α , a tube voltage 40 kV and tube current 25 mA).

Functional groups of GO, LDH, and hybrid layered NS of LDH@GO were analyzed by FTIR spectrophotometer (FTIR-8000 Spectrophotometer, Shimadzu, Tokyo, Japan). The number of scans per sample was kept 25 and resolution of the measurements was kept at 4 cm⁻¹. The recorded wave number range was kept in the range of 500-4000 cm⁻¹.

Surface morphology and EDS mapping of GO, LDH and hybrid layered NS of LDH@GO were determined by using field emission scanning electron microscope (FE-SEM, S-4800 Hitachi, Tokyo, Japan) operated at an accelerating voltage of 30 kV and transmission electron microscope (TEM, Philips CM-200, Eindhoven, The Netherlands) with 75 μ A of filament current and 200 kV of accelerating voltage. For analyzing elemental composition of LDH@GO, EDS spectra were recorded on spectrometer attached with the FE-SEM.

Thermal stability of GO, LDH, and hybrid layered NS of LDH@GO was determined by a thermo gravimetric analyzer (TGA-50, Shimadzu, Tokyo, Japan). Powder form of all samples was used for thermal analysis. TGA was recorded at room temperature. Approximately 10 mg of sample was placed in a platinum pan for TGA analysis. The temperature range was kept from 30 to 700°C and a heating rate was kept 10°C/min under nitrogen atmosphere to avoid thermoxidative degradation.

3. Results and discussion

3.1 Structural and crystallinity analysis

The crystal structure as well as orientation were studied from XRD analysis which also verified the average spacing between GO, LDH, hybrid layered NS of LDH@GO. Fig. 1 and Fig. S4 show the XRD patterns of GO, uncalcined LDH, calcined LDH, modified LDH and hybrid layered NS of LDH@GO. From Fig. 1 (a), it can be seen that the diffraction peak of exfoliated GO was recorded at $2\theta = 10.11^\circ$, which attributes to the plane of GO (002) features basal spacing of 8.73 Å. This also shows the complete oxidation of graphite into the GO due to the introduction of oxygen-containing functional groups on the graphene sheets (Lonkar et al., 2015). The characteristic peaks are appeared as sharp in the XRD patterns of uncalcined LDH (Fig. S4) the peaks at $2\theta = 11.7^\circ, 23.5^\circ, 34.9^\circ, 39.5^\circ, 47.1^\circ, 60.9^\circ$ and 62.4° which are corresponding to the (003) (006) (012) (015) (018) (110) (113) planes. The XRD pattern of calcined LDH (Fig. 1b) shows weak reflections, confirms the destruction of layered structure upon calcinations and formation of metals oxides. From XRD pattern of (Fig. 1(c)), an intercalation of SDS anions could be seen after modification with SDS due to virtue of an increase in basal spacing. Hence peak shifted slightly towards lower diffraction angle (Chakraborty et al., 2014). This also indicates the expansion in the interlayer distance and these planes also

show the characteristic peaks of Mg/Al based LDH (Lonkar et al., 2013; Yang et al., 2014; Zazoua et al., 2014). The XRD patterns (Fig. 1d) of the as-prepared LDH@GO hybrid NS show amorphous nature, but no characteristic peak of GO was observed in hybrid layered NS of LDH@GO. The peaks at 34.0° and 60.0° , at (012) and (110) intensities correspond to LDH. The peak of GO at $2\theta = 10.11^\circ$ (002), shown in Fig. 1(a), was significantly broadened and shifted towards lower diffraction angle because of increased distance between GO sheets due to incorporation of exfoliated LDH (Latorre-Sanchez et al., 2012; Lonkar et al., 2015).

3.2 Functional group analysis

The FT-IR spectra of GO, calcined LDH, modified LDH and hybrid layered NS of LDH@GO are shown in Fig. 2(a-d). The strong and broad peak at 3360 cm^{-1} seen in Fig. 2(a) indicates the presence of surface O-H stretching due to vibrations of the H-O-H groups of water. The other peak corresponds to oxygen functional groups, such as carboxyl (C=O) stretching of COOH groups (1725 cm^{-1}), aromatic (C=C) stretching (1615 cm^{-1}), epoxy (C-O) group stretching (1218 cm^{-1}) and alkoxy (C-OH) group stretching vibrations (1043 cm^{-1}) (Wen et al., 2013; Esmaeili et al., 2014; Low et al., 2015). The FTIR spectrum of the calcined LDH (Fig. 2b) displays the broad and strong bands in the range of $3200\text{-}3600\text{ cm}^{-1}$ and the other low frequency region (800 cm^{-1}) is attributed to metal-oxygen and metal-hydroxyl vibration modes present in the lattice of LDH. The FTIR spectrum of the modified LDH (Fig. 2c) shows two types of bands; first is corresponding to the anionic species of SDS intercalated and second is corresponding to the pristine LDH. It also shows the stretching band for aliphatic CH_3 of the long chain of SDS molecules around $2854\text{-}2965\text{ cm}^{-1}$. The bands at 1216 and 1063 cm^{-1} are ascribed to the symmetric vibration of sulfate from SDS, respectively (Chakraborty et al., 2014; Jain et al., 2016). The other low frequency regions (800 cm^{-1})

are attributed to metal–oxygen and metal–hydroxyl vibration modes present in the lattice of LDH. (Yang et al.,2014).The broad band in the range of 3200–3700 cm^{-1} may be due to presence of O-H stretching vibration of hydrogen bonded metal hydroxide layer and interlayer water molecules(Lonkar et al., 2013; Chakraborty et al., 2014; Zazoua et al.,2014). The band observed near 1637 cm^{-1} is assigned to the bending vibration of water molecules. From the peak intensities corresponding to GO and LDH shown in Fig. 2(d), it can be said that carbonyl, epoxide, and ether groups were observed to be weakened in the FTIR spectrum of LDH@GO hybrids. This also confirms the formation of hybrid nanostructures. Moreover, the XRD patterns (Fig. 1 d) and TEM images (Fig. 4 c and Fig. 4d) confirm the inter layer exfoliated hybridization.

3.3 Surface morphology and elemental analysis

Typical FE-SEM and TEM images of GO, calcined LDH, modified LDH and LDH@GO hybrid NS are shown in Fig. 3 and Fig. 4. GO exhibited the exfoliated layers structure with scrolled multilayer sheets with thin, transparent, smooth, wrinkles and folding on the basal and edges with an average 50 nm in thickness and up to the certain μm in length (Fig.3a and Fig.4a)(Oraon et al., 2015; Jain et al., 2016; Kavinkumaret al., 2016, Pérez del Pino et al., 2016; Yan et al., 2016;). The GO sheets are generally exfoliated due to ultrasonic vibrations and LDH are get intercalated in between GO sheets. As shown in Fig. 3(c) and Fig. 4(b), the LDH consist of regular and thin hexagonal single platelets with exfoliated structures with an average thickness of 25 nm and length up to the 250nm, also indicate size and morphology at nanoscale (Chakraborty et al., 2012; Diao et al., 2014) as compared to calcined LDH shown in Fig. 3(b) and also TEM images of LDH are inserted in Fig.4(b).

The surface morphology of the hybrid NS of LDH@GO was also studied by FE-SEM, TEM (Fig. 3(d), and Fig. 4(c-d)). The corresponding images show significant

morphological differences with respect to the GO. Based on microscopic and XRD (Fig. 1c) analysis of hybrid NS of LDH@GO, it can be considered that LDH has been uniformly inserted into GO sheets and considerably amplifies the distances between adjacent GO sheets (Scheme 1) (Zhao et al., 2014, Lonkar et al., 2015; Kang et al., 2016; Kavinkumaret al., 2016; Zhang et al., 2016). According to morphological results, a schematic representation of the formation of LDH@GO hybrid NS material is shown in Scheme 1. LDH is positively charged ions and GO with a basal spacing at nanoscale could be considered as a negatively charged single sheet of graphene due to the presence of carboxylate. The LDH nanoplatelets are adsorbed on the surface of GO nanosheets due to the electrostatic interaction between GO and LDH. The intercalation of LDH into the nanosheets of graphene can effectively prevent the restacking of GO nanosheets (Zhao et al., 2014).

Formation of hybrid NS of LDH@GO was further confirmed by EDS analysis, which showed presence of these different elements such as C, O, Mg and Al peaks as well as their relative quantities (Fig. 3e). The EDS spectra as well as elemental mapping of GO, LDH and LDH@GO further confirms the presence of LDH incorporated in GO sheets (Fig. S1, Fig. S2 and Fig. S3 given in supplementary information).

3.4 Thermal behavior

The TGA behaviors of the GO, LDH and hybrid NS of LDH@GO are displayed in Fig. 5. The pristine GO exhibits single step degradation with significant mass loss at around 180°C due to the pyrolysis of the labile oxygen-containing functional groups. The presence of the oxygen functional groups makes GO thermally unstable, as it undergoes pyrolysis at elevated temperatures (Fig. 5a), mass loss was recorded up to 90% below 200°C mainly due to the decomposition of oxygen-containing groups and the loss of interlayer water molecules (Esmaeili et al., 2014). The modified LDH show typical two

stage thermal decomposition pattern with 45% mass loss (Fig. 5b). The consecutive loss of water present in the LDH was observed from room temperature to 200°C, chemisorbed at 200–360°C and the water arising from the dehydroxylation of the layers at 225–450°C. The TGA pattern of hybrid NS of LDH@GO with 67% mass loss (Fig. 5c), shows three major mass loss stages. The first mass loss observed at approximately 210°C, is attributed to the removal of loosely bound water molecules from the LDH interlayer. The second mass loss, in the temperature range 250–350°C, is due to the removal of oxygen functionalities. The third and final mass loss was observed above temperature of 350°C, which is primarily due to dehydroxylation and decarbonation of the LDH sheets (Lonkar et al., 2015) and thus the TGA graph showed 22 % GO hybrid with LDH.

4. Conclusion

Hybrid layered NS of LDH@GO were synthesized by an efficient and rapid bath ultrasonic technique. The resulting hybrid layered NS of LDH@GO showed improvement in spacing between the GO sheets. Moreover, the hybrid layered NS of LDH@GO demonstrated good thermal stability as compared to pristine GO. Hence, conjunction of GO and LDH hybrid NS endow the multifunctional properties in a single hybrid system. The effectiveness of the method described the synthesis of LDH@GO hybrid layered NS and can be useful for the preparation of other graphene-based hybrid NS. Similarly, the use of bath ultra-sonication provided proper exfoliation of GO sheets for the development of multi-functional hybrid layered NS. An increased distance between GO sheets and improved thermal stability suggest that LDH nanoplatelets may be incorporated in between GO sheets during bath sonication. Further studies on the relationship between the solution reflux casting of hybrid layered NS of LDH@GO and

their intercalation and exfoliation mechanisms in polymer matrices along with their detailed investigations of the physico-mechanical (multifunctional) properties are future prospective of this work.

Acknowledgement

Prashant S. Khobragade is thankful and gratefully acknowledge to the University Grant Commission (UGC), New Delhi, Government of India for providing Rajiv Gandhi National Junior Research Fellowship [F1-17.1/2014-15/RGNF-2014-15-SC-MAH-58232/(SA-III/Website)]. Department of Science and Technology (DST-UKIERI), New Delhi, India [File No: DST/INT, UK/P-108/2014] is also acknowledged for financial support to carry out this research work.

References

- Acharya, H., Srivastava, S.K. and Bhowmick, A.K., 2007. Synthesis of partially exfoliated EPDM/LDH nanocomposites by solution intercalation: structural characterization and properties. *Compos. Sci. Technol.*, 67, 2807–2816.
- Alsharaehn, E., Mussa, Y., Ahmed, F., Aldawsari, Y., Hindawi, M.A., and Sing, G.K., 2016. Novel route for the preparation of cobalt oxide nanoparticles/reduced graphene oxide nanocomposites and their antibacterial activities. *Ceramics Int.*, 42, 3407–3410.
- Angelopoulou, A., Voulgari, E., Diamanti, E.K., Gournis, D. and Avgoustakis, K., 2015. Graphene oxide stabilized by PLA–PEG copolymers for the controlled delivery of paclitaxel. *European J. Pharmac. Biopharmac.*, 93, 18–26.
- Basu, D., Das, A., Stöckelhuber, K.W., Wagenknecht, U. and Heinrich, G., 2014. Advances in layered double hydroxide (LDH)-based elastomer composites. *Prog. Polym. Sci.*, 39, 594–626.

Bouakaz, B.S., Pillin, I., Habi, A. and Grohens, Y., 2015. Synergy between fillers in organomontmorillonite/graphene–PLA nanocomposites. *Appl. Clay Sci.*, 116,69–77.

Bourlinos, A.B., Georgakilas, V., Zboril, R., Steriotis, T.A. and Stubos, A.K., 2009. Liquid-phase exfoliation of graphite towards solubilized graphenes. *Small*, 5,1841–1845.

Chakraborty, M., Dasgupta, S., Sengupta, S., Chakraborty, J., Ghosh, S., Ghosh, J., Mitra, M.K., Mishra, A., Mandal, T.K. and Basu, D., 2012. A facile synthetic strategy for Mg–Al layered double hydroxide material as nanocarrier for methotrexate. *Ceramics Int.*, 38,941–949.

Chakraborty, S., Kumar, M., Suresh, K. and Pugazhenti, G., 2014. Influence of organically modified Ni Al layered double hydroxide (LDH) loading on the rheological properties of poly (methyl methacrylate)(PMMA)/LDH blend solution. *Powder Technol.*, 256, 196–203.

Chatterjee A. and Mishra, S., 2013. Nano-calcium carbonate (CaCO₃)/Polystyrene (PS) core-shell nanoparticle: It's effect on physical and mechanical properties of high impact polystyrene (HIPS). *J. Polym. Res.*, 20, 249.

Chatterjee A., Mishra, S., 2013. Rheological, thermal and mechanical properties of nano-calcium carbonate (CaCO₃)/Poly(methyl methacrylate) (PMMA) core-shell nanoparticles reinforced polypropylene (pp) composites. *Macromol. Res.*, 21,474–483.

Chen, H., He, Y.Y., Lin, M.H., Lin, S.R., Chang, T.W., Lin, C.F., Yu, C.T.R., Sheud M.L., Chen, C.B. and Lin Y.S., 2016. Characterizations of zinc oxide nanorods incorporating a graphene layer as antibacterial nanocomposites on silicon substrates. *Ceramics Int.*, 42,3424–3428.

Das, T.K. and Prusty, S., 2013. Graphene-based polymer composites and their applications. *Polym. Plast. Technol. Eng.*, 52,319–331.

Esmaili, A. and Entezari, M.H., 2014. Facile and fast synthesis of graphene oxide nanosheets via bath ultrasonic irradiation. *J. Coll.Interf. Sci.*, 432, 19–25.

Gallastegui, A.G., Iruretagoyena, D., Gouvea, V., Mokhtar, M., Asiri, A.M., Basahel, S.N., Al-Thabaiti, S.A., Alyoubi, A.O., Chadwick, D. and Shaffer, M.S.P., 2012. Graphene oxide as support for layered double hydroxides: enhancing the CO₂ adsorption capacity. *Chem. Mater.*, 24,4531–4539.

Hansora, D.P., Shimpi, N.G., Mishra, S., 2015. Graphite to graphene via graphene oxide: An overview on synthesis, properties, and applications. *JOM*, 67, 2855–2868.

He, R. and Hen, W., 2016. Ultrasonic assisted synthesis of TiO₂-reduced graphene oxide nanocomposites with superior photovoltaic and photocatalytic activities. *Ceramics Int.*, 42, 5766–5771.

Jain R., Mishra S., 2016. Electrical and electrochemical properties of graphene modulated through surface functionalization. *RSC Adv*, 6, 27404–27415.

Kang, X.J., Zhang, J.M., Sun, X.W., Zhang, F.R. and Zhang, Y.X., 2016. One-Pot synthesis of vanadium dioxide nano flower son graphene oxide. *Ceramics Int.*, 42, pp. 7883–7887.

Kavinkumar, T. and Manivannan, S., 2016. Uniform decoration of silver nanoparticle on exfoliated graphene oxide sheets and its ammonia gas detection. *Ceramics Int.*, 42, 1769–1776.

Ladewig, K., Niebert, M., Xu, Z.P., Gray, P.P. and Lu, G.Q.M., 2010. Controlled preparation of layered double hydroxide nanoparticles and their application as gene delivery vehicles. *Appl. Clay Sci.*, 48, 280–289.

Latorre-Sanchez, M., Atienzar, P., Abellán, G., Puche, M., Fornés, V., Ribera, A. and García, H., 2012. The synthesis of a hybrid graphene–nickel/manganese mixed oxide and its performance in lithium-ion batteries. *Carbon*, 50, 518–525.

- Lonkar, S.P., Kutlu, B., Leuteritz, A. and Heinrich, G., 2013. Nanohybrids of phenolic antioxidant intercalated into MgAl-layered double hydroxide clay. *Appl. Clay Sci.*, 71,8–14.
- Lonkar, S.P., Raquez, J.M. and Dubois, P., 2015. One-pot microwave-assisted synthesis of graphene/layered double hydroxide (LDH) nanohybrids. *Nano-Micro Lett.*, 7, 332–340.
- Low, F.W., Lai, C.W. and Hamid, S.B.A., 2015. Easy preparation of ultrathin reduced graphene oxide sheets at a high stirring speed. *Ceramics Int.*, 41, 5798–5806.
- Mali, A.D., Shimpi N.G., and Mishra S.,2014. Thermal, mechanical and morphological properties of surface-modified montmorillonite-reinforced Viton rubber nanocomposites. *Polym. Int.*,63, 338–346.
- Menezes, J., Da Silva, T., Dos Santos, J., Catari, E., Meneghetti, M., Da Matta, C., Alexandre-Moreira, M., Santos-Magalhães, N., Grillo, L. and Dornelas, C., 2014. Layered double hydroxides (LDH) as carrier of antimony aimed for improving leishmaniasis chemotherapy. *Appl. Clay Sci.*,91,127–134.
- Mishra S., Shimpi N.G., Mali, A.D., 2012. Investigation of photo-oxidative effect on morphology and degradation of mechanical and physical properties of nano CaCO₃silicone rubber composites. *Polym. Adv. Technol.*,23,236–246.
- Mishra S., Shimpi N.G., Mali, A.D., 2012. Surface modification of montmorillonite (MMT) using column chromatography technique and its application in silicone rubber nanocomposites. *Macromol. Res.*, 20,44–50.
- Mishra, S., Chatterjee A., Singh, R.P.2011. Novel synthesis of nano-calcium carbonate(CaCO₃)/polystyrene (PS) core–shell nanoparticles by atomized microemulsion technique and its effect on properties of polypropylene (PP) composites. *Polym. Adv. Technol.*, 22,2571–2582.

- Nandi, D., Gupta, K., Ghosh, A.K., De, A., Ray, N.R. and Ghosh, U.C., 2013. Thermally stable polypyrrole–Mn doped Fe (III) oxide nanocomposite sandwiched in graphene layer: Synthesis, characterization with tunable electrical conductivity. *Chem. Eng. J.*, 220,107–116.
- Olf, H.W., Torres-Dorante, L.O., Eckelt, R. and Kosslick, H., 2009. Comparison of different synthesis routes for Mg–Al layered double hydroxides (LDH): characterization of the structural phases and anion exchange properties. *Appl. Clay Sci.*, 43, 459–464.
- Oraon, R., De Adhikari, A., Tiwari, S.K., Sahu, T.S. and Nayak, G.C., 2015. Fabrication of nanoclay based graphene/polypyrrolenanocomposite: An efficient ternary electrode material for high performance supercapacitor. *Appl. Clay Sci.*, 118,231–238.
- Pino, A.P., Datcu, A. and György, E., 2016. Direct multipulse laser processing of titanium oxide–graphene oxide nanocomposite thin films. *Ceramics Int.*, 42, 7278–7283.
- Sun, Y., Zhou, J., Cai, W., Zhao, R. and Yuan, J., 2015. Hierarchically porous NiAl-LDH nanoparticles as highly efficient adsorbent for p-nitrophenol from water. *App. Surf. Sci.*, 349, 897–903.
- Tang, Z., Chen, H., Chen, X., Wu, L. and Yu, X., 2012. Graphene oxide based recyclable dehydrogenation of ammonia borane within a hybrid nanostructure. *J Am. Chem. Soc.*, 134, 5464–5467.
- Wen, T., Wu, X., Tan, X., Wang, X. and Xu, A., 2013. One-pot synthesis of water-swelling Mg–Al layered double hydroxides and graphene oxide nanocomposites for efficient removal of As (V) from aqueous solutions. *ACS Appl. Mater. Interf.*, 5, 3304–3311.

Wu, Z.S., Zhou, G., Yin, L.C., Ren, W., Li, F. and Cheng, H. M., 2011. Graphene/metal oxide composite electrode materials for energy storage. *Nano Energy*, 1, 107–131.

Yadav, M., Rhee, K.Y. and Park, S.J., 2014. Synthesis and characterization of graphene oxide/carboxymethylcellulose/alginate composite blend films. *Carbohydr.Polym.*,110, 18–25.

Yan, Q., Liu, Q. and Wang, J., 2016. A simple and fast microwave assisted approach for the reduction of graphene oxide. *Ceramics Int.*, 42, 3007–3013.

Yan, S., He, P., Ji, D., Yang, Z., Duan, X., Wang, S., Zhou, Y., 2016. Effect of reduced graphene oxide content on the microstructure and mechanical properties of graphene–geopolymernanocomposites.*Ceramics Int.*,42, 752–758.

Yang, K., Yan, L.G., Yang, Y.M., Yu, S.J., Shan, R.R., Yu, H.Q., Zhu, B.C. and Du, B., 2014. Adsorptive removal of phosphate by Mg–Al and Zn–Al layered double hydroxides: Kinetics, isotherms and mechanisms. *Sep. Purif. Technol.*, 124, 36–42.

Yang, Y., Fan, G. and Li, F., 2014. Synthesis of novel marigold-like carbonate-type Mg–Al Layered double hydroxide micro-nanostructures via a two-step intercalation route. *Mater.Lett.*, 116, 203–205.

Yuan, Y. and Shi, W., 2012. A novel LDH nanofiller intercalated by silsesquioxane for preparing organic/inorganic hybrid composites. *Appl. Clay Sci.*, 67, 83–90.

Z., Zhou, Lin, Y., Yao, S. and Yan H., 2016, Preparation of calcium carbonate@graphene oxide core–shell microspheres in ethylene glycol for drug delivery. *Ceramics Int.*, 42,2281–2288.

Zazoua, H., Saadi, A., Bachari, K., Halliche, D. and Rabia, C., 2014. Synthesis and characterization of Mg–M (M: Al, Fe, Cr) layered double hydroxides and their application in the hydrogenation of benzaldehyde. *Res.Chem.Intermed.*, 40, 931–946.

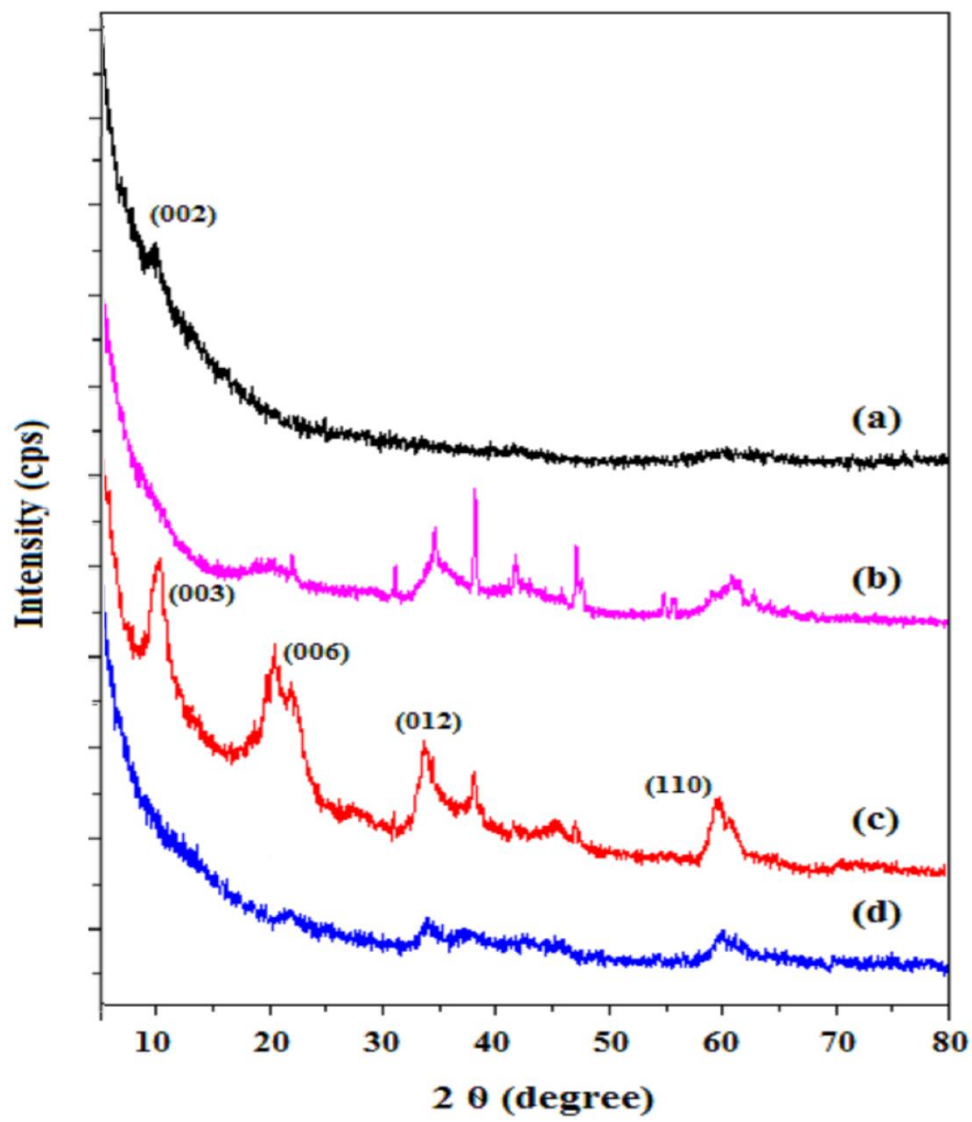
Zhang, L., He, Y., Feng, S., Zhang, L., Zhang, L., Jiao, Z., Zhan, Y. and Wang Y., 2016. Preparation and tribological properties of novel boehmite/graphene oxide nano-hybrids. *Ceramics Int.*, 42, 6178–6186.

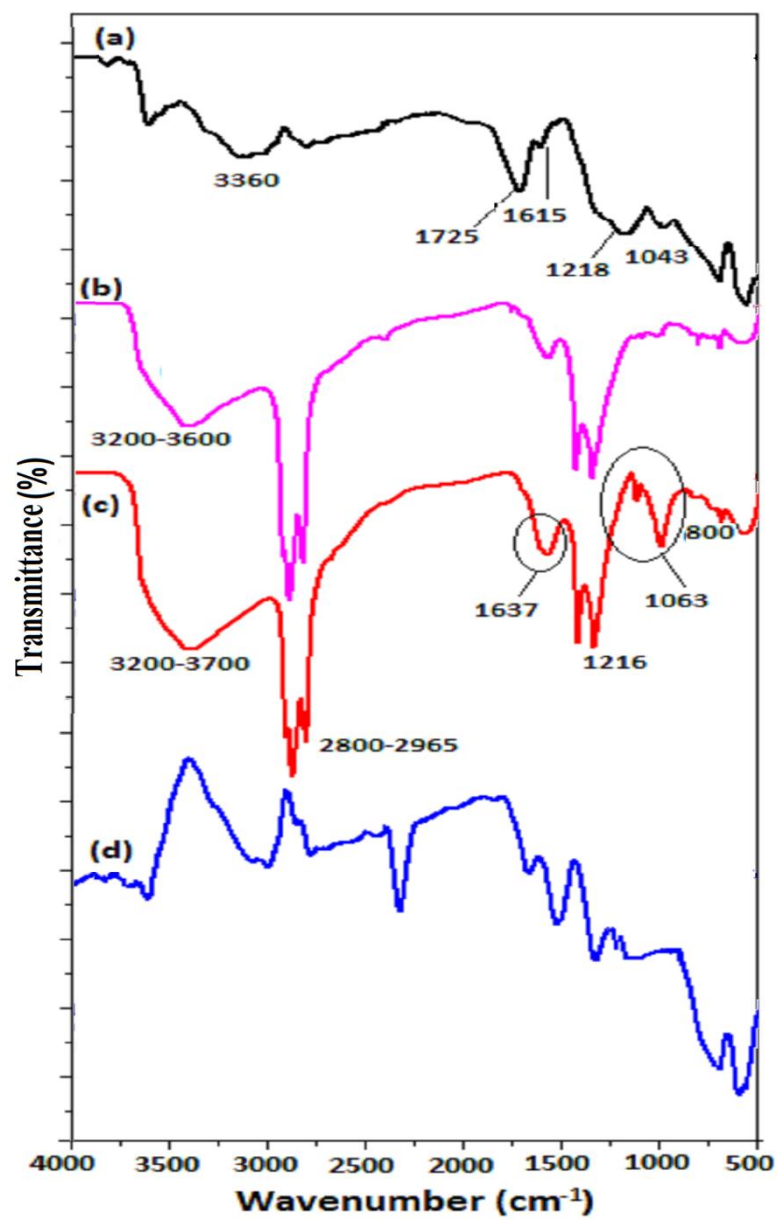
Zhao, H., Qiu, F., Yan, J., Wang, J., Li, X. and Yang, D., 2016. Preparation of economical and environmentally friendly graphene/palygorskite/TiO₂ composites and its application for the removal of methylene blue. *Appl. Clay Sci.*, 121, 137–145.

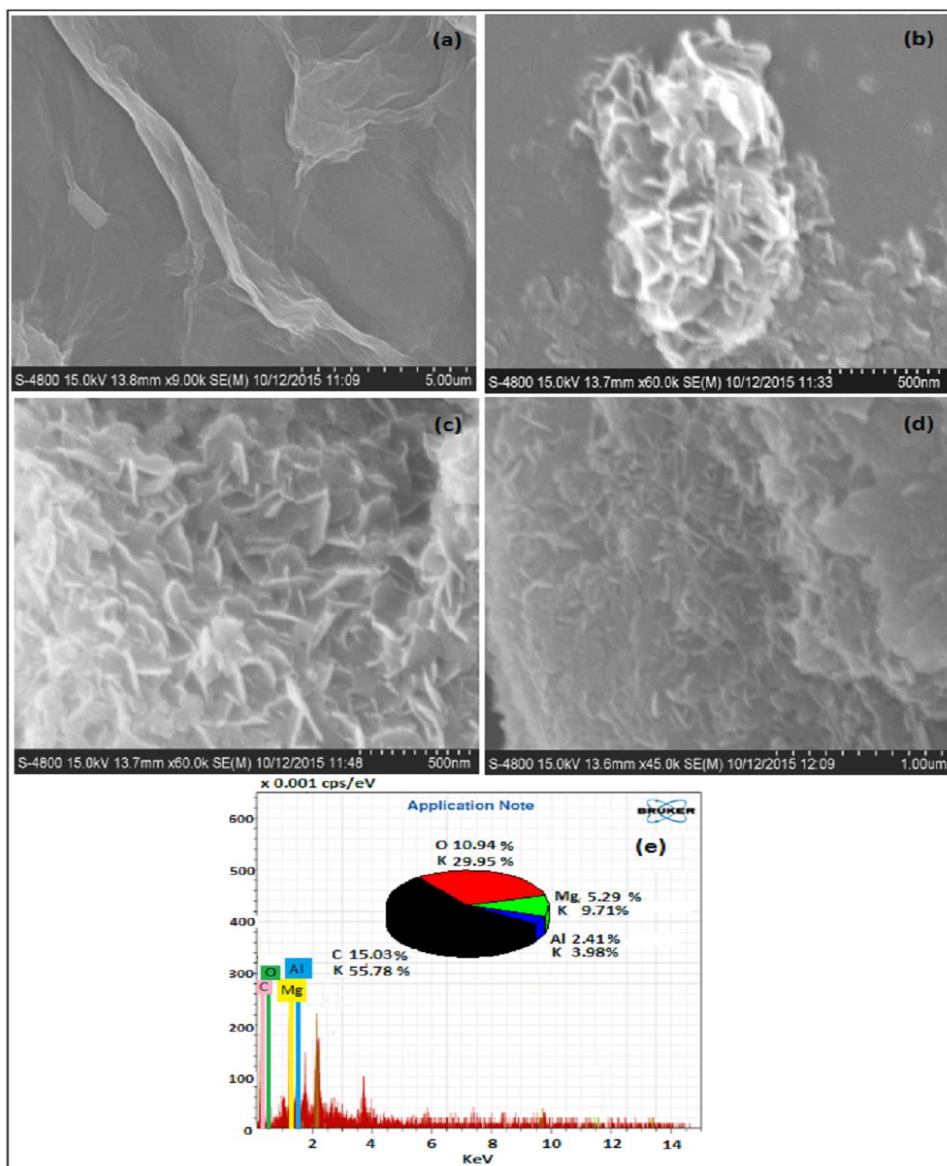
X. Zhao, J.P. Cao, J. Zhao, G.H. Hu, Z.M. Dang, 2014. A hybrid Mg-Al layered double hydroxide/graphene nanostructure obtained via hydrothermal synthesis. *Chem. Phys. Lett.*, 605–606, 77–80.

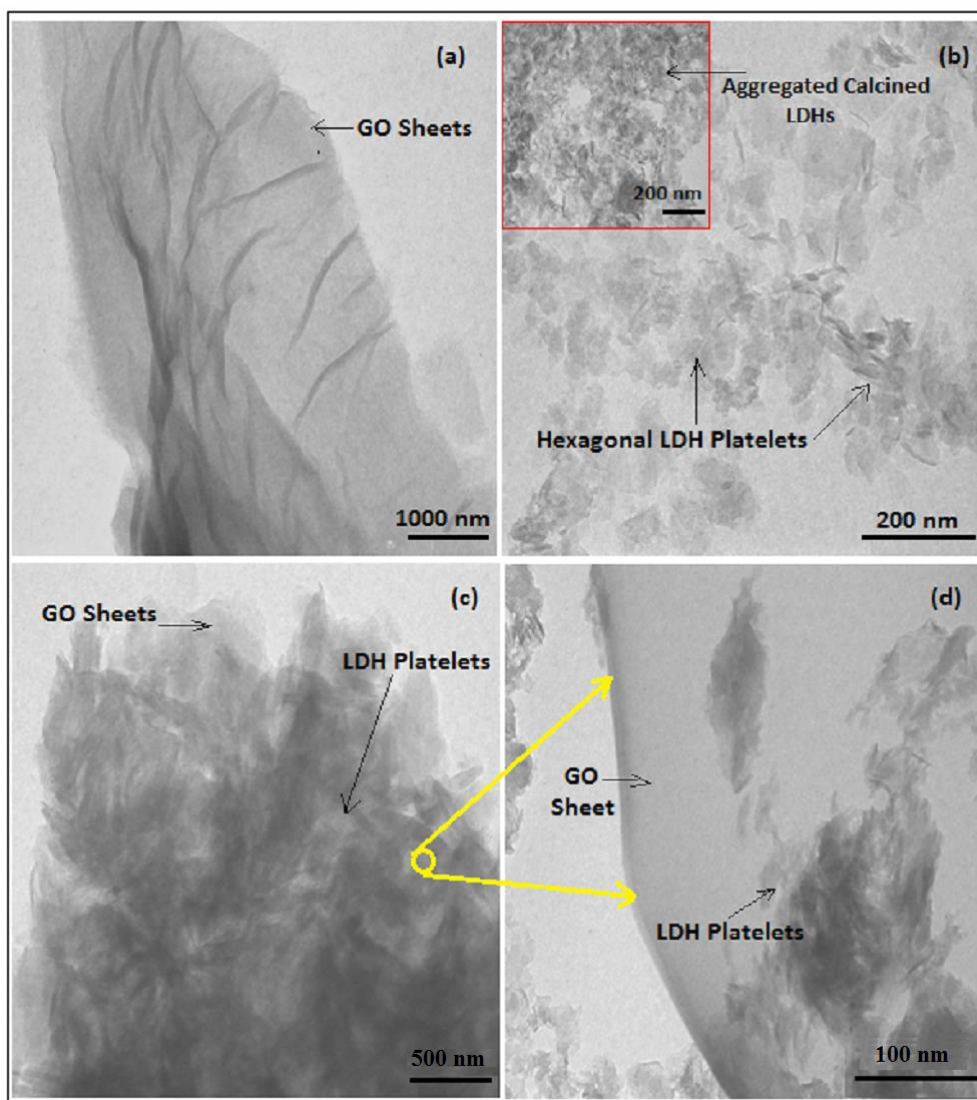
Captions for Figures

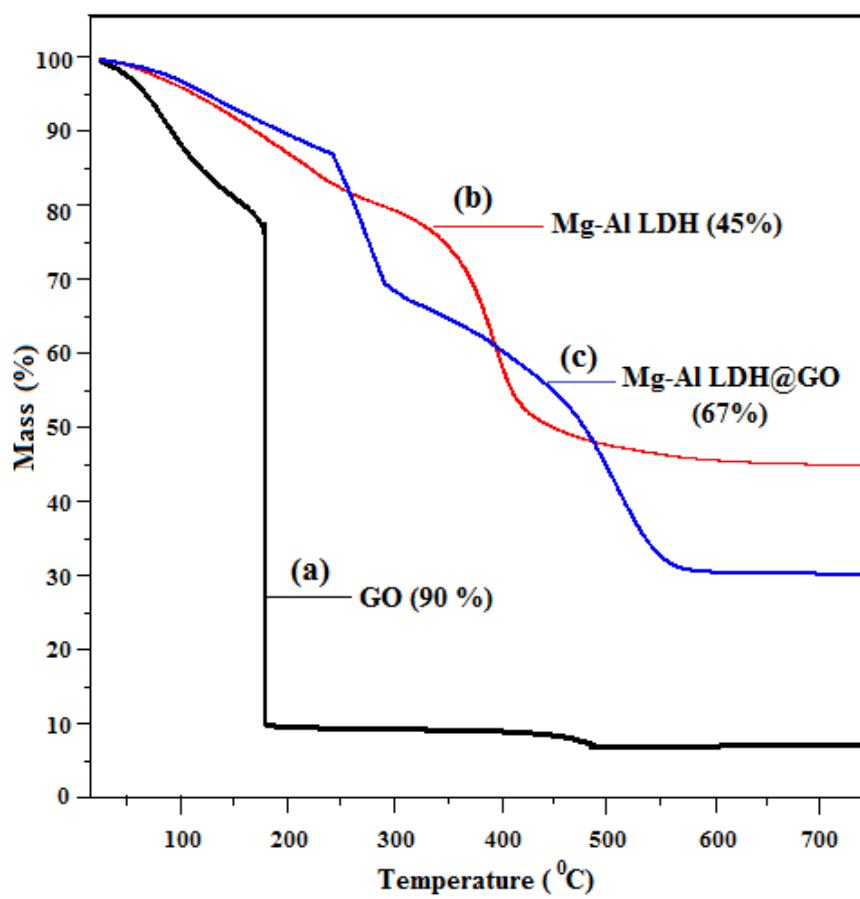
- Fig. 1.** XRD diffraction pattern of (a) GO (b) Calcined Mg-Al LDH (c) Modified Mg-Al LDH (d) Hybrid layeredNS of Mg-Al-LDH@GO.
- Fig. 2** FTIR spectra of (a) GO (b) Calcined Mg-Al LDH (c) ModifiedMg-Al LDH (d) Hybrid layeredNSof Mg-Al-LDH@GO.
- Fig. 3.** FE-SEM images of, (a) GO (b) Calcined Mg-Al LDH (c) Modified Mg-Al LDH (d) Hybrid layeredNS of Mg-Al-LDH@GO (e) Elemental analysis of Mg-Al-LDH/@GO based nanostructures.
- Fig. 4.** TEM images of (a) GO (b) Mg-Al LDH (c-d) Hybrid layeredNS of Mg-Al-LDH@GO.
- Fig. 5.** TGA curves of (a) GO (b) modified Mg-Al LDH (c) Mg-Al-LDH@GObased hybrid nanostructures.
- Scheme 1.** Pictorial representation of the formation of interlayer hybrid layered nanostructures of Mg-Al-LDH/@GO prepared by bath ultrasonication technique.

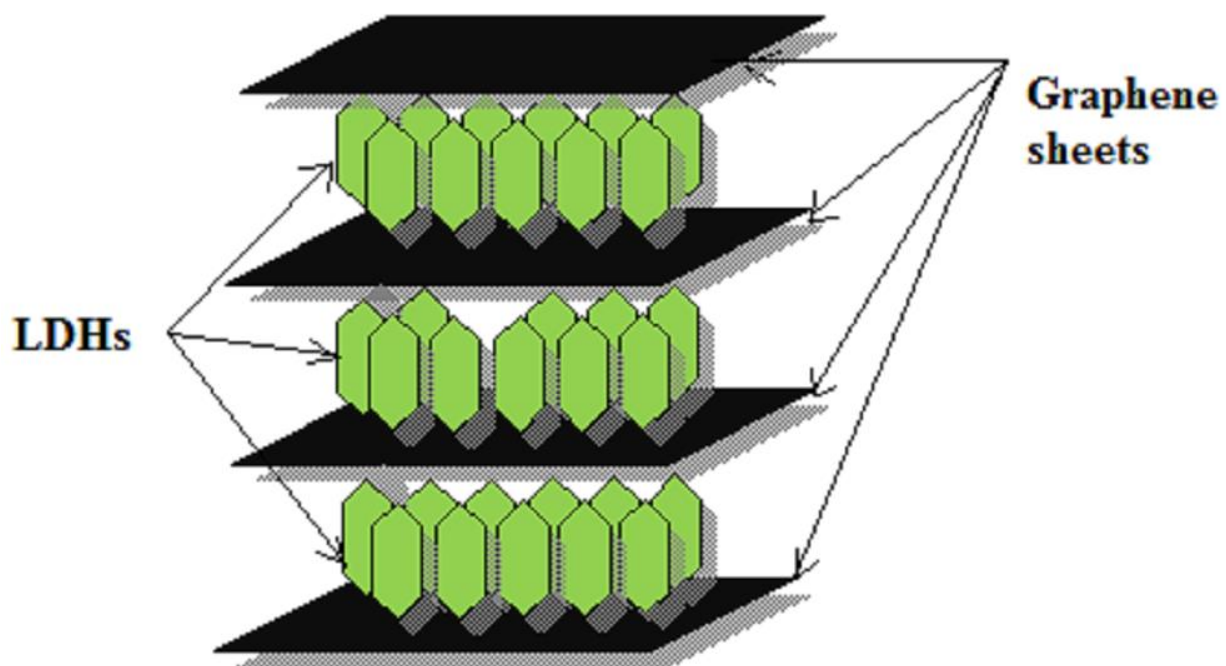












Intercalation of LDHs in between exfoliated graphene sheets

Supplementary Information

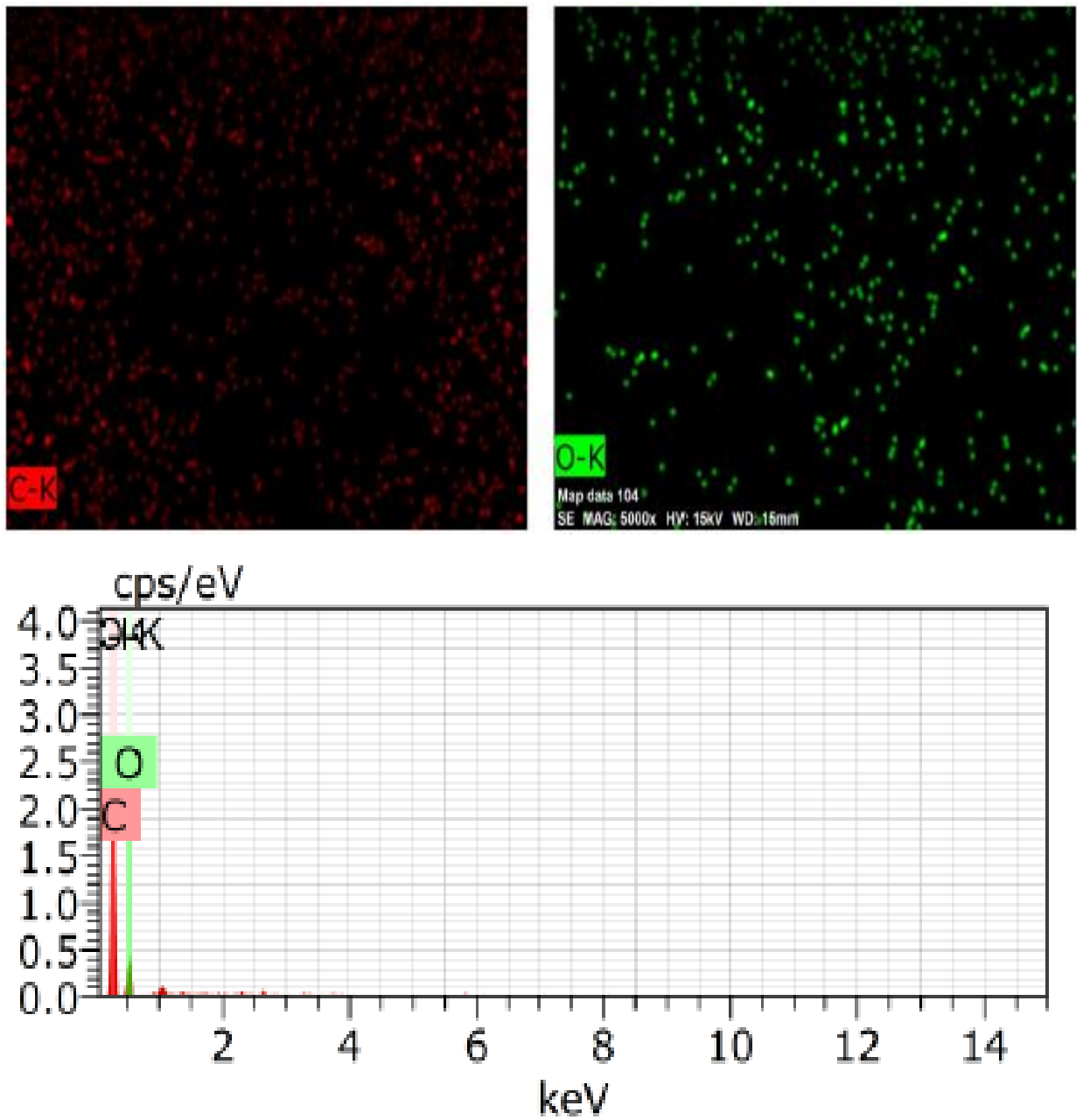


Fig. S1. FE-SEM EDS and Elemental mapping spectrum analysis indicating corresponding elemental mapping C and O in GO.

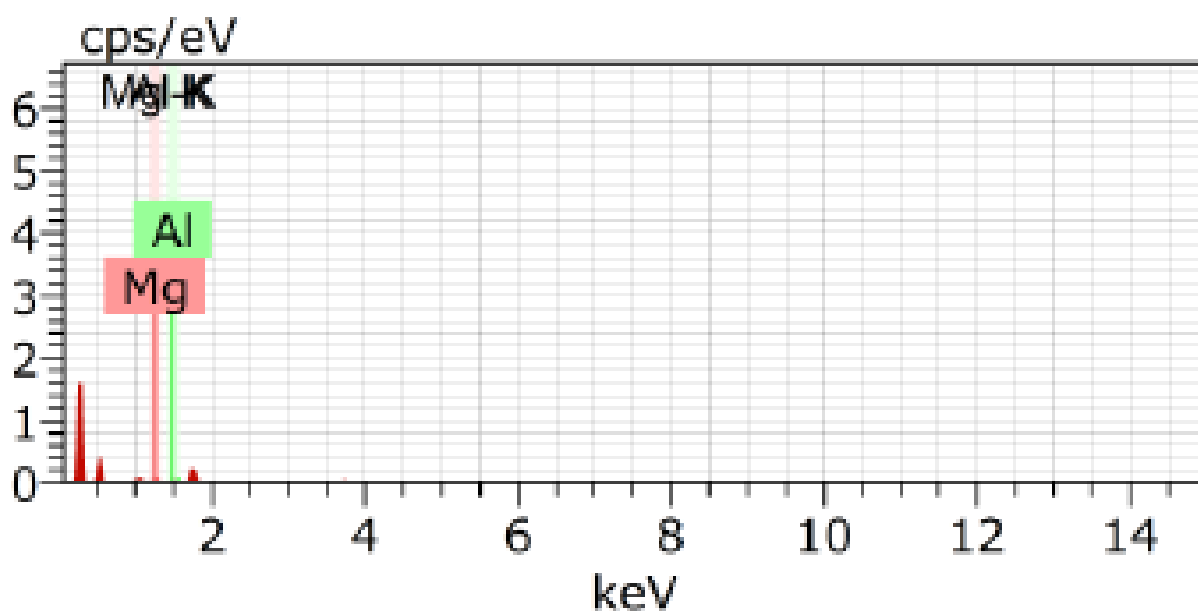
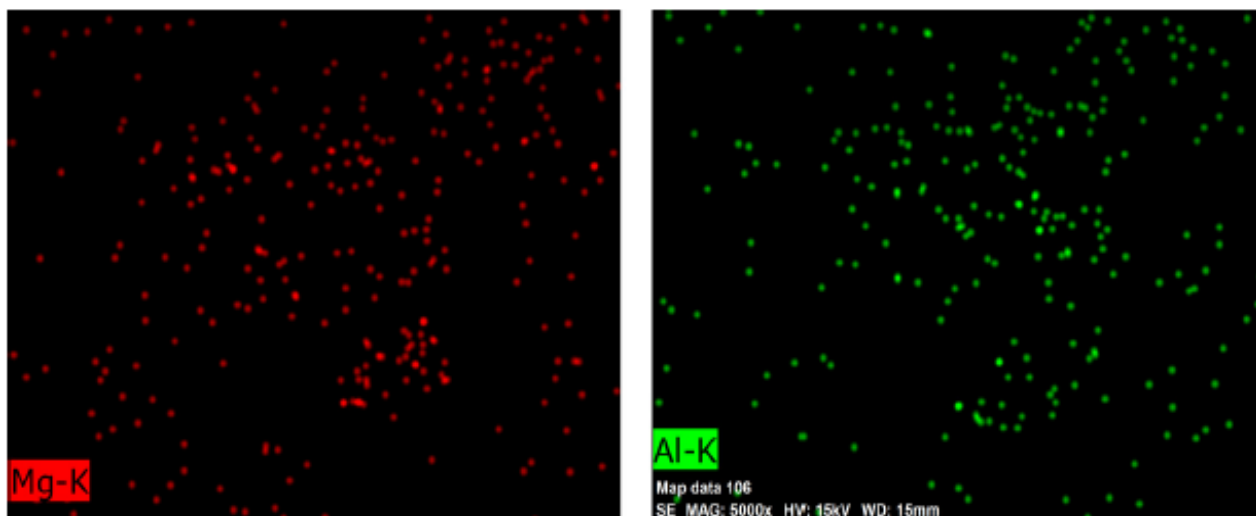


Fig. S2. FE-SEM EDS and Elemental mapping spectrum analysis indicating corresponding elemental mapping of Mg and Al in Mg-Al LDH.

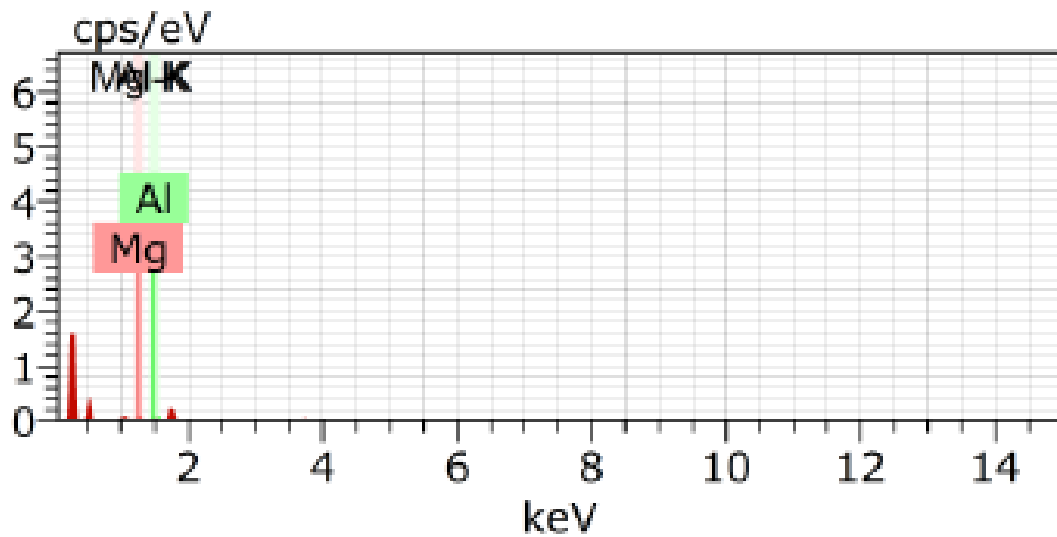
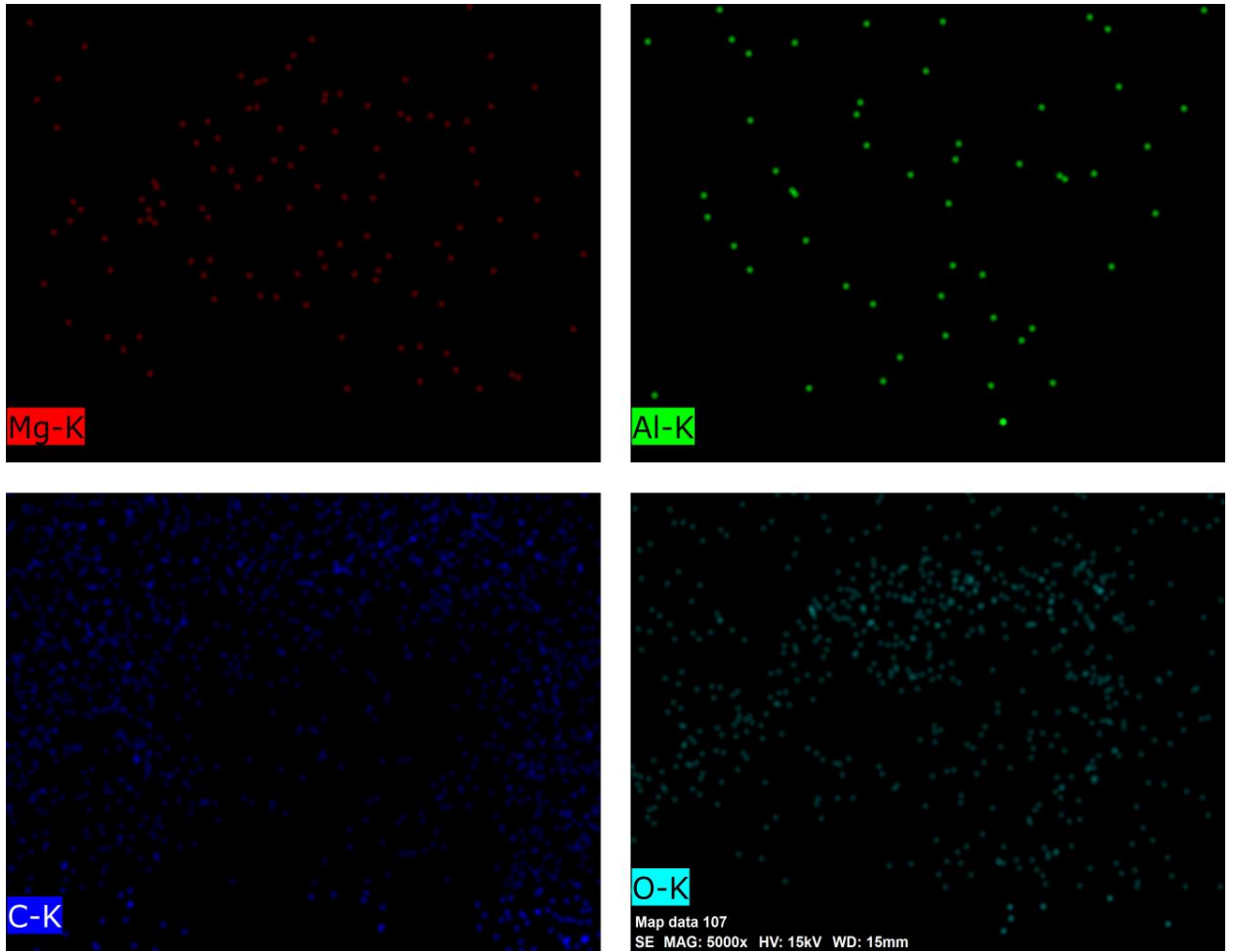


Fig. S3. FE-SEM EDS and Elemental mapping spectrum analysis indicating corresponding elemental mapping C, O, Mg and Al in hybrid NS of LDH@GO.

FE-SEM EDS pattern and elemental mapping of GO, LDH and hybrid NSs of LDH@GO was shown in Fig. S1, S2 and Fig. S3. The carbon and oxygen distribution in the plane of graphene indicates highly homogeneous, as can be seen by the elemental mapping shown in Fig. S1. The same C, and O mapping of graphene suggests that not only the edge but also the plane of graphene contain a large amount of C and O functionalities. Similarly, magnesium and aluminum distribution in Mg-Al-LDH can be seen from the by the elemental mapping shown in Fig. S2, which indicates that LDH contain sufficient amount of Mg and Al. The EDX spectra as well as elemental mapping of and LDH@GO further confirms the presence of LDHs incorporated in GO sheets C and O for GO, Mg and Al for LDH and C, O, Mg and Al for LDH@GO hybrid nanostructures, respectively (Fig. S3). The images (Fig. S3) also suggest that the LDH are homogeneously inserted/ distribution in GO sheets. And EDX pattern describes the presence of LDH in GO sheets.

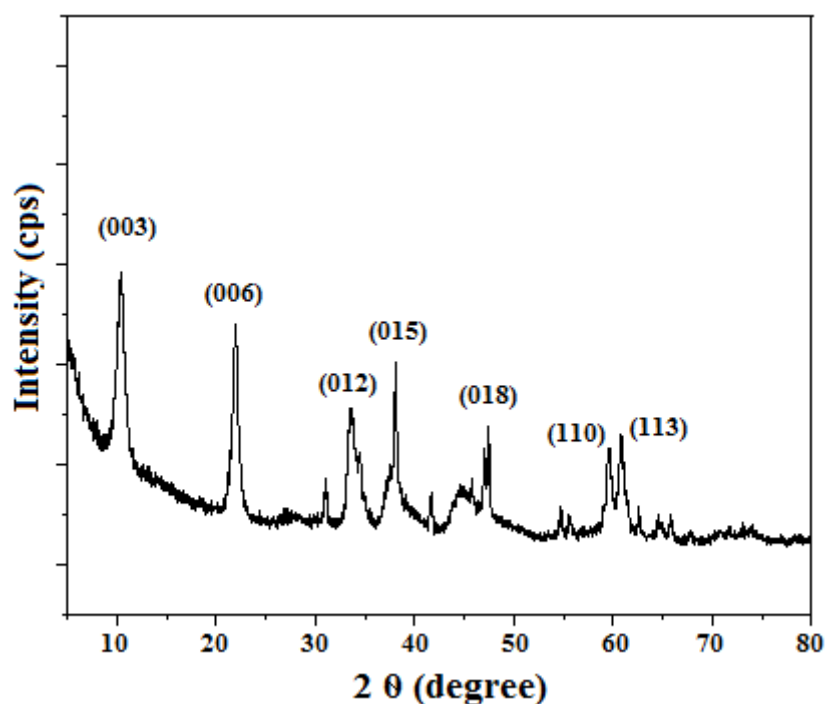


Fig. S4. XRD diffraction pattern of uncalcined Mg-Al LDH

The characteristic peaks are appeared as sharp in the XRD patterns of uncalcined LDH (Fig. S4) the peaks at $2\theta = 11.7, 23.5, 34.9, 39.5, 47.1, 60.9$ and 62.4° which are corresponding to the (003) (006) (012) (015) (018) (110) (113) planes and these planes also show the characteristic peaks of Mg-Al-LDH